Facile Synthesis of $Ba_{1-x}K_xFe_2As_2$ Superconductors via Hydride Route

Julia V. Zaikina,[†,‡ *] Maria Batuk,[&] Artem Abakumov,[&] Alexandra Navrotsky,[‡] and Susan M. Kauzlarich[†*]

[†] Department of Chemistry and [‡]Peter A. Rock Thermochemistry Laboratory and NEAT ORU, University of California at Davis, One Shields Avenue, Davis, California 95616, United States

[&] EMAT, University of Antwerp, Groenenborgerlaan 171, B-2020 Belgium

Supporting Information

Table S1. Data collection and refinement parameters for the Rietveld refinement of $Ba_{1-x}K_xFe_2As_2$ samples using synchrotron radiation (11-BM at the Advanced Photon Source, Argonne National Laboratory).

Sample ID	S # 2 x = 0	S # 2 x = 0	S # 16 x = 0.2	S # 16 x = 0.2
Composition	$BaFe_2As_2$	$BaFe_2As_2$	$Ba_{0.84}K_{0.16(3)}Fe_2As_2$ FeAs (5.6 wt. %)	$Ba_{0.84}K_{0.16(1)}Fe_2As_2$ FeAs (8.0 wt. %)
Space group	*I*4/*mmm*	*Fmmm*	*I*4/*mmm*	*Fmmm*
***T* / K**	295	100	295	100
***a*, Å** ***b*, Å** ***c*, Å**	3.9614(1) = *a* 13.0216(3)	5.6139(1) 5.5746(1) 12.9594(3)	3.9452(1) = *a* 13.1322(7)	5.5864(2) 5.5564(2) 13.061(6)
V, Å^3	204.3(5)	405.571(1)	204.395(7)	405.41(4)
λ, Å	0.41383			
ρ, g/cm^3	6.481	6.53	5.809	7.012
μ, mm^{-1}	7.316	7.372	6.471	7.386
2θ, degrees	$0.5 \leq 2\theta \leq$ 49.989			
R_p	9.3	8.7	10.1	9.3
R_{wp}	12.5	12.1	13.3	12.6
R_{exp}	8.7	9.0	7.1	9.0
χ^2	2.09	1.82	3.5	1.97
Sample ID	S # 12 x = 0.7	S # 13 x = 0.5	S#10 x = 1	S#9 x = 1
Composition	$Ba_{0.32}K_{0.68(1)}Fe_2As_2$	$Ba_{0.52}K_{0.48(2)}Fe_2As_2$	$K_{0.98(1)}Fe_2As_2$	$KFe_{1.9(6)}As_2$
Space group	*I*4/*mmm*			
***T* / K**	295			
***a*, Å** ***b*, Å** ***c*, Å**	3.8832(1) = *a* 13.5381(8)	3.9068(1) = *a* 13.3743(1)	3.847(2) = *a* 13.884(3)	3.849(2) = *a* 13.867(3)
V, Å^3	204.15(2)	204.127(8)	205.42(16)	205.38(16)
λ, Å	0.41383			
ρ, g/cm^3	5.8158	5.816	4.859	4.86
μ, mm^{-1}	6.479	6.48	5.281	5.282
2θ, degrees	$0.5 \leq 2\theta \leq$ 49.989			
R_p	12.1	9.7	8.4	8.9
R_{wp}	16.6	13.1	11.4	12.4
R_{exp}	9.1	8.2	8.8	9.4
χ^2	3.30	2.60	1.66	1.76

Table S2. Synthesis conditions and phase fractions from Rietveld refinement of powder XRD data.

Sample #	Molar ratios	Annealing temperature*	**Major phase*** and impurity (content of impurity, wt.%)
$BaFe_2As_2$			
S#1	$BaH_2/FeAs$ = 1/2	hand-grinding 900°C	**$BaFe_2As_2$**, FeAs (15) $BaO{\cdot}xH_2O$
S#2	$BaH_2/FeAs$ = 1/2	900°C	**$BaFe_2As_2$**
S#3	$BaH_2/FeAs$ = 1.1/2	700°C	**$BaFe_2As_2$,** FeAs (5)
S#4	$BaH_2/Fe/As$ = 1.1/2/2	900°C	**$BaFe_2As_2$,** FeAs (5)
S#5	$BaH_2/Fe/As$ = 1.2/2/2	900°C	**$BaFe_2As_2$**
KFe_2As_2			
S#5	KH/FeAs = 1/2	900°C	**KFe_2As_2,** Fe_2As (5), FeAs (3)
S#6	KH/FeAs = 1.1/2	900°C	**KFe_2As_2,** Fe_2As (10), K_3As
S#7	KH/FeAs =1/2	700°C	**KFe_2As_2,** FeAs (20) and oxidation products ($KAsO_3$ and $Fe_2O_3{\cdot}xH_2O$)
S#8	KH/FeAs = 1.2/2	700°C	**KFe_2As_2,** FeAs (2) and oxidation products ($KAsO_3$ and $Fe_2O_3{\bullet}xH_2O$)
S#9	KH/FeAs = 1.3/2	700°C	**KFe_2As_2**
S#10	KH/FeAs = 1.3/2	500°C	**KFe_2As_2**
	KH/Fe/As = 1.3/2/2	700°C	**KFe_2As_2**
$Ba_{1.1(1-x)}K_{1.3x}Fe_2As_2$ (0 < x < 1) with FeAs as precursor			
S#11	BaH_2/KH/FeAs = 0.11/1.17/2 x = 0.9	700°C	**$Ba_{0.13}K_{0.87}Fe_2As_2$**
S#12	BaH_2/KH/FeAs = 0.33/0.91/2 x = 0.7	700°C	**$Ba_{0.32}K_{0.68}Fe_2As_2$**
S#13	BaH_2/KH/FeAs = 0.55/0.65/2 x = 0.5	700°C	**$Ba_{0.46}K_{0.54}Fe_2As_2$**
S#14	BaH_2/KH/FeAs = 0.66/0.52/2 x = 0.4	700°C	**$Ba_{0.65}K_{0.35}Fe_2As_2$** FeAs (7)
S#15	BaH_2/KH/FeAs = 0.77/0.39/2 x = 0.3	700°C	**$Ba_{0.77}K_{0.23}Fe_2As_2$** FeAs (6), Fe_2As(2)
S#16	BaH_2/KH/FeAs = 0.88/0.26/2 x = 0.2	700°C	**$Ba_{0.88}K_{0.12}Fe_2As_2$** FeAs (7)
S#17	BaH_2/KH/FeAs = 0.88/0.26/2 x = 0.2	900°C	**$Ba_{0.90}K_{0.10}Fe_2As_2$** Fe_2As (4)
$Ba_{1.1(1-x)}K_{1.3x}Fe_2As_2$ (0 < x < 1) with elemental Fe and As as precursors			
S#18	BaH_2/KH/Fe/As = 0.33/0.91/2/2 x = 0.7	700°C	**$Ba_{0.28}K_{0.65}Fe_2As_2$** Fe_2As (3)
S#19	BaH_2/KH/Fe/As = 0.55/0.65/2/2 x = 0.5	700°C	**$Ba_{0.47}K_{0.52}Fe_2As_2$** Fe_2As (6)
S#20	BaH_2/KH/Fe/As = 0.77/0.39/2/2 x = 0.3	700°C	**$Ba_{0.78}K_{0.22}Fe_2As_2$** Fe_2As (5)

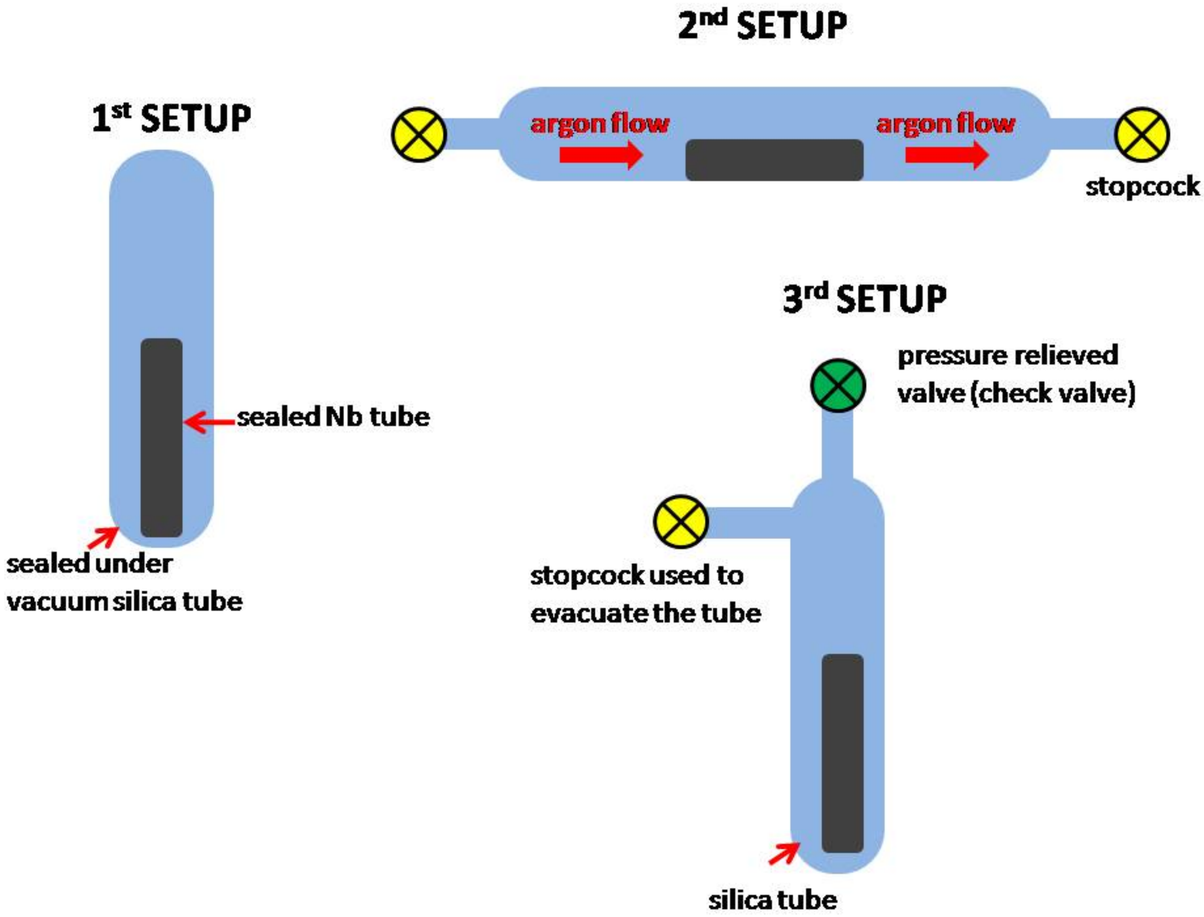

Figure S1. Different setups used for annealing of $Ba_{1-x}K_xFe_2As_2$ samples sealed into Nb tube.

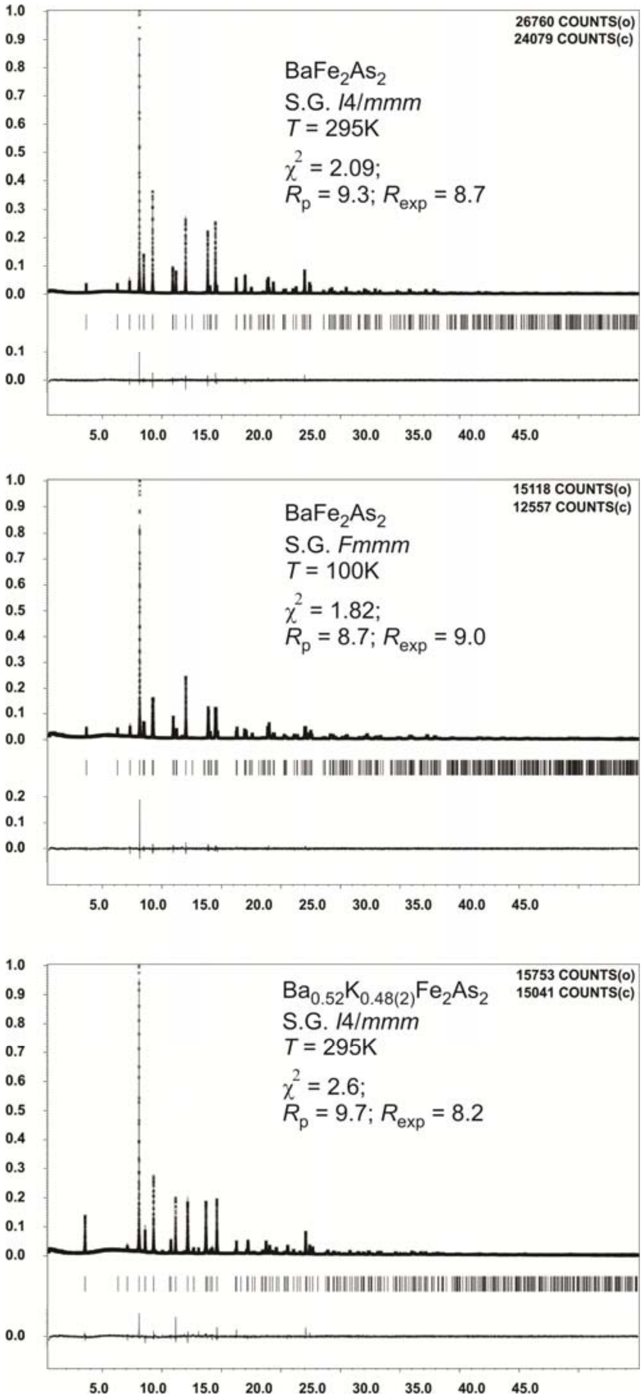

Figure S2. Powder XRD patterns and corresponding Rietveld refinements (black line) of the PXRD data (black dots) for $BaFe_2As_2$ collected at room temperature (top) and 100 K (middle) and $Ba_{0.52}K_{0.48(2)}Fe_2As_2$ at room temperature (bottom). Black marks indicate the theoretical Bragg peak positions. The difference is shown as a curve at the bottom.

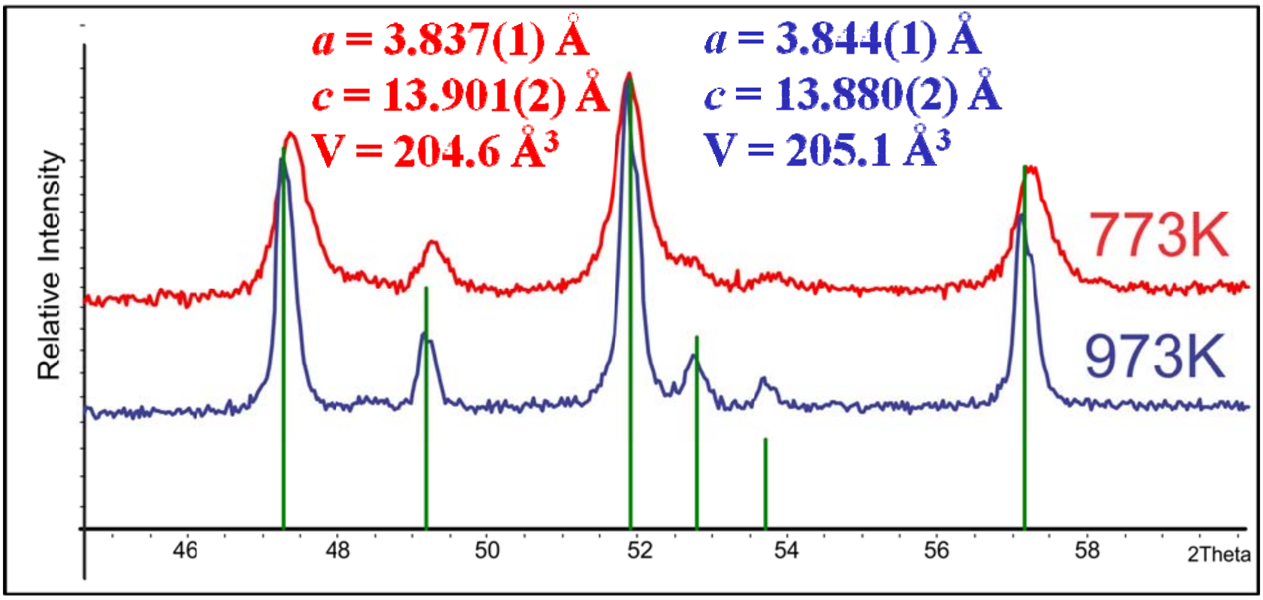

Figure S3. Powder X-ray diffraction powder patterns for the samples of KFe_2As_2 prepared at 500°C (red) and 700°C (blue). In green: theoretical X-ray diffraction pattern for KFe_2As_2.

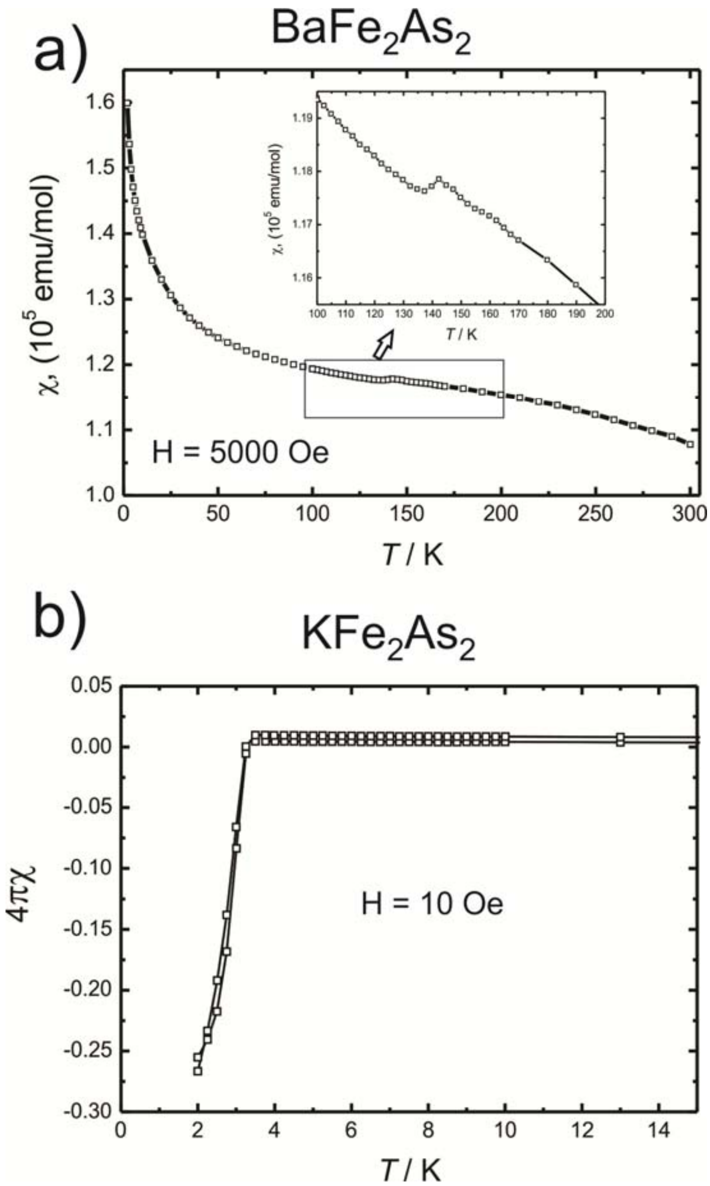

Figure S4. a) Temperature dependence of magnetic susceptibility, $\chi(T)$ = M/H measured in an applied field of 5000 Oe for $BaFe_2As_2$ sample; Insert: $\chi(T)$ in the 100 K -200 K; the kink at ~140 K corresponds to the structural and magnetic phase transition (spin-density wave transition) [Rotter, M.; Tegel, M.; Johrendt, D. *Phys. Rev. Lett*. **2008**, *101*, 4.]

b) Temperature dependence of magnetic susceptibility, $\chi(T)$ = M/H, measured in an applied field of 10 Oe for KFe_2As_2 sample; a well-defined drop at 3.5 K for both ZFC and FC curves is indicative of the onset of superconducting transition. The superconducting volume fraction was estimated to be approximately 27%.

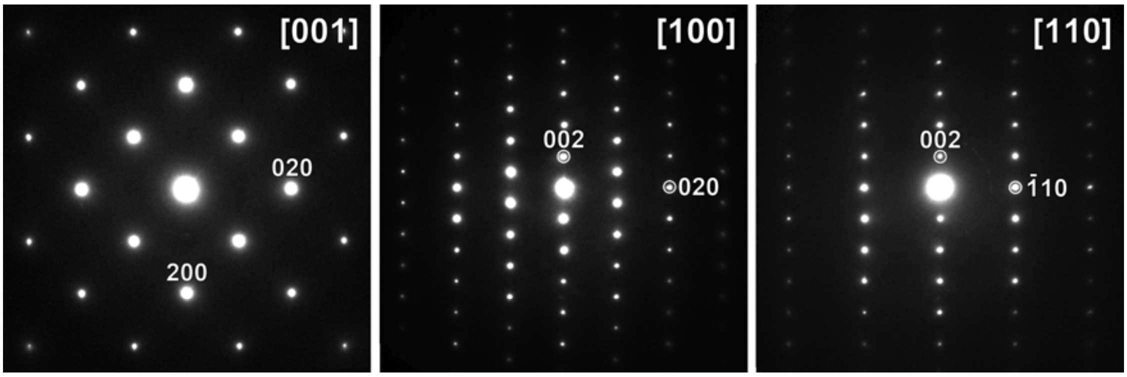

Figure S5. ED patterns along the main crystallographic axes of the $Ba_{0.6}K_{0.4}Fe_2As_2$ structure.

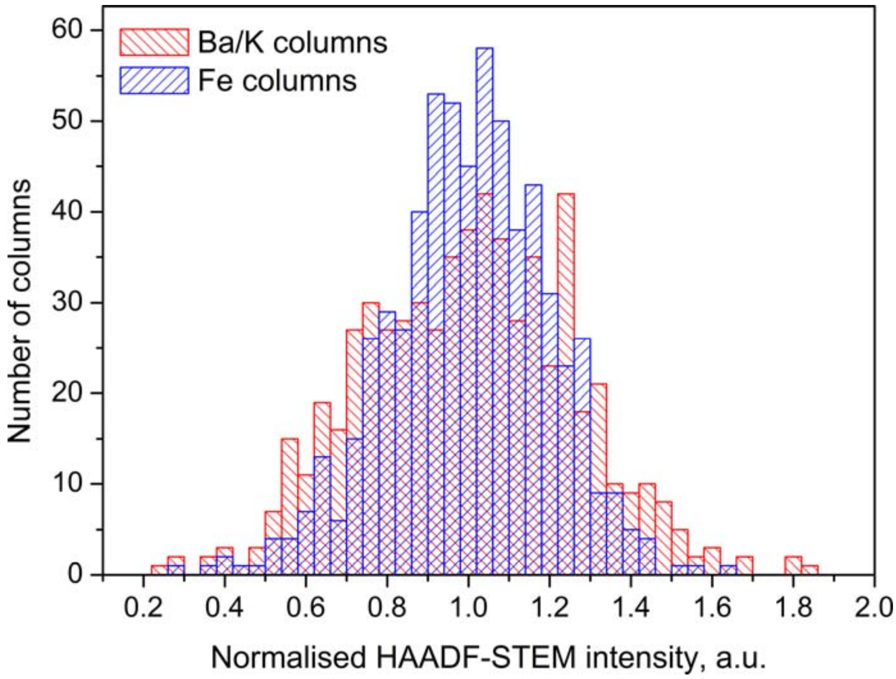

Figure S6. Intensity distribution of the Ba/K (red) and Fe (blue) columns measured from the [110] HAADF-STEM image of $Ba_{0.5}K_{0.5}Fe_2As_2$. Both distributions were fitted with Gaussian function. The values of full width at half maximum (FWHM) are 0.60 for the distribution measured on Ba/K columns and 0.43 for Fe columns.

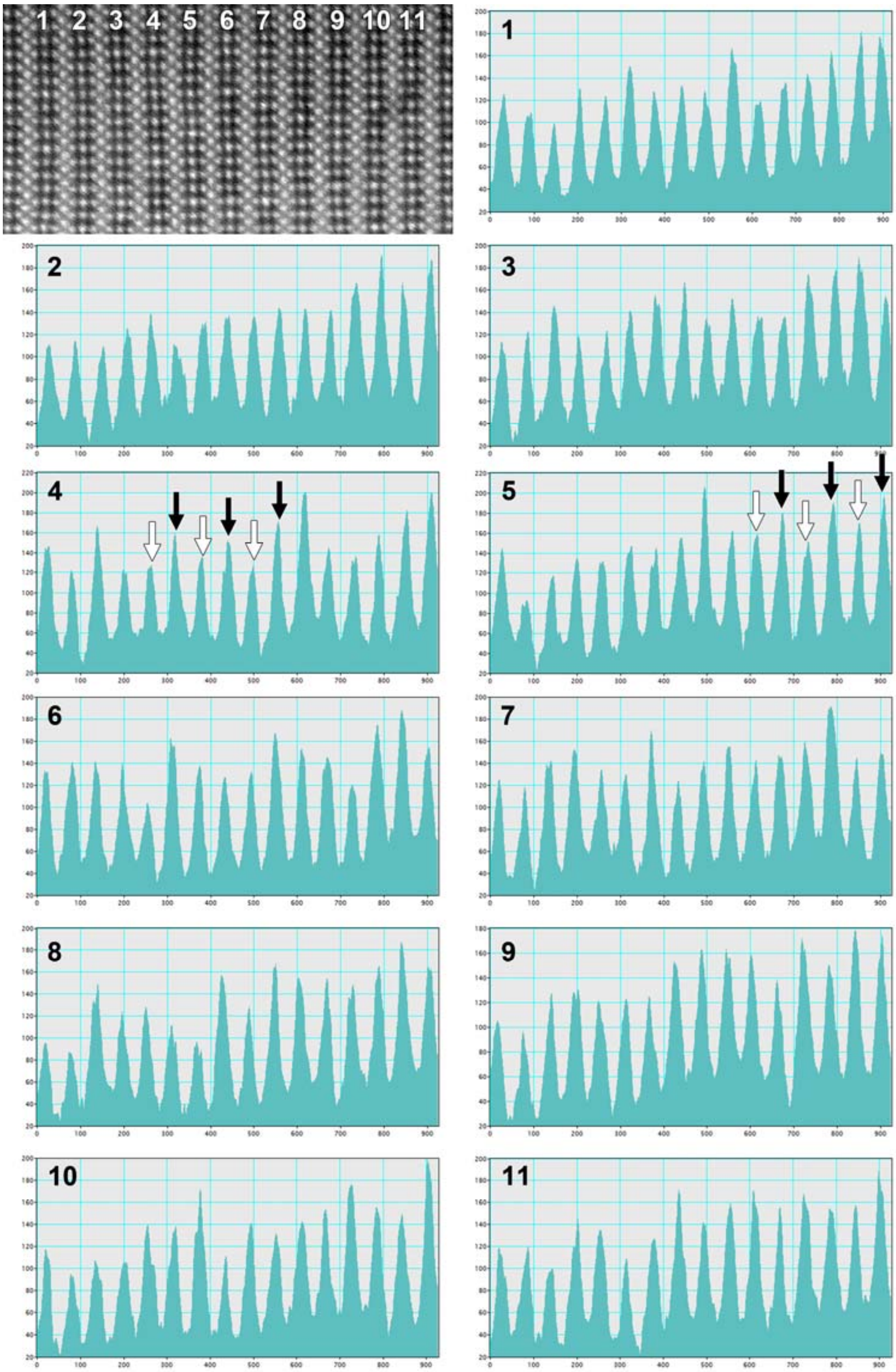

Figure S7. Enlarged [110] HAADF-STEM image for the $Ba_{0.5}K_{0.5}Fe_2As_2$ sample with marked layers 1-11 and the corresponding intensity profiles measured along these layers. In the layers 4 and 5 one can notice alternation between Ba-enriched and Ba-depleted columns, whereas in the rest of the layers their distribution seems to be random.

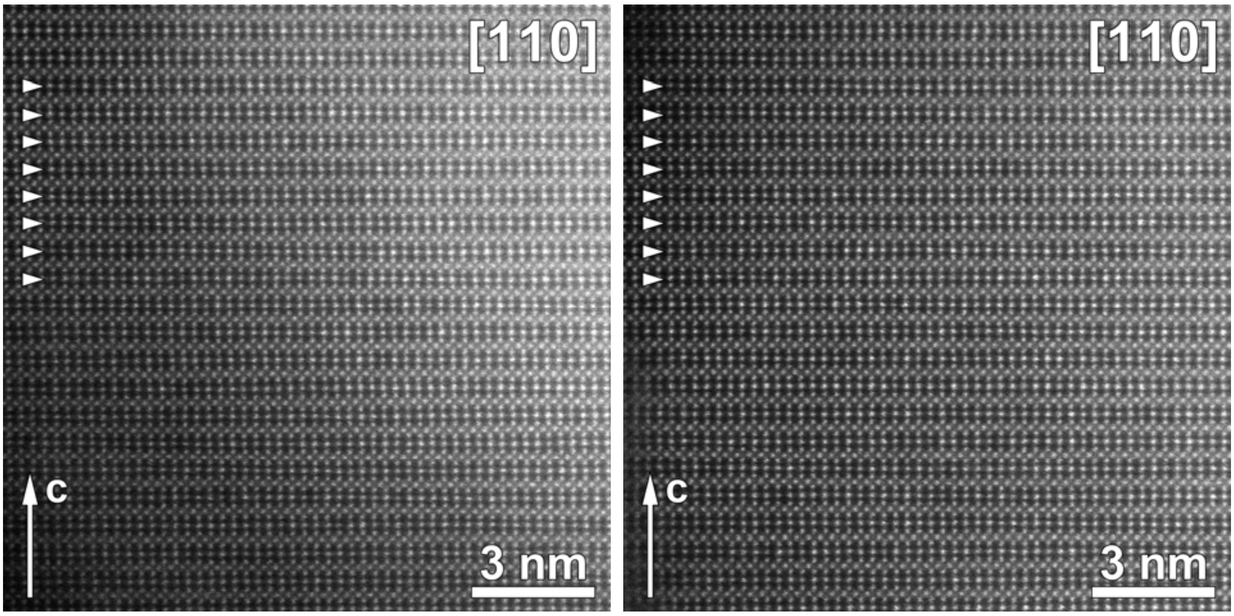

Figure S8. HAADF-STEM images for the $Ba_{0.6}K_{0.4}Fe_2As_2$ sample taken along [110] zone axis. Arrowheads indicate the Ba/K layers in the structure.

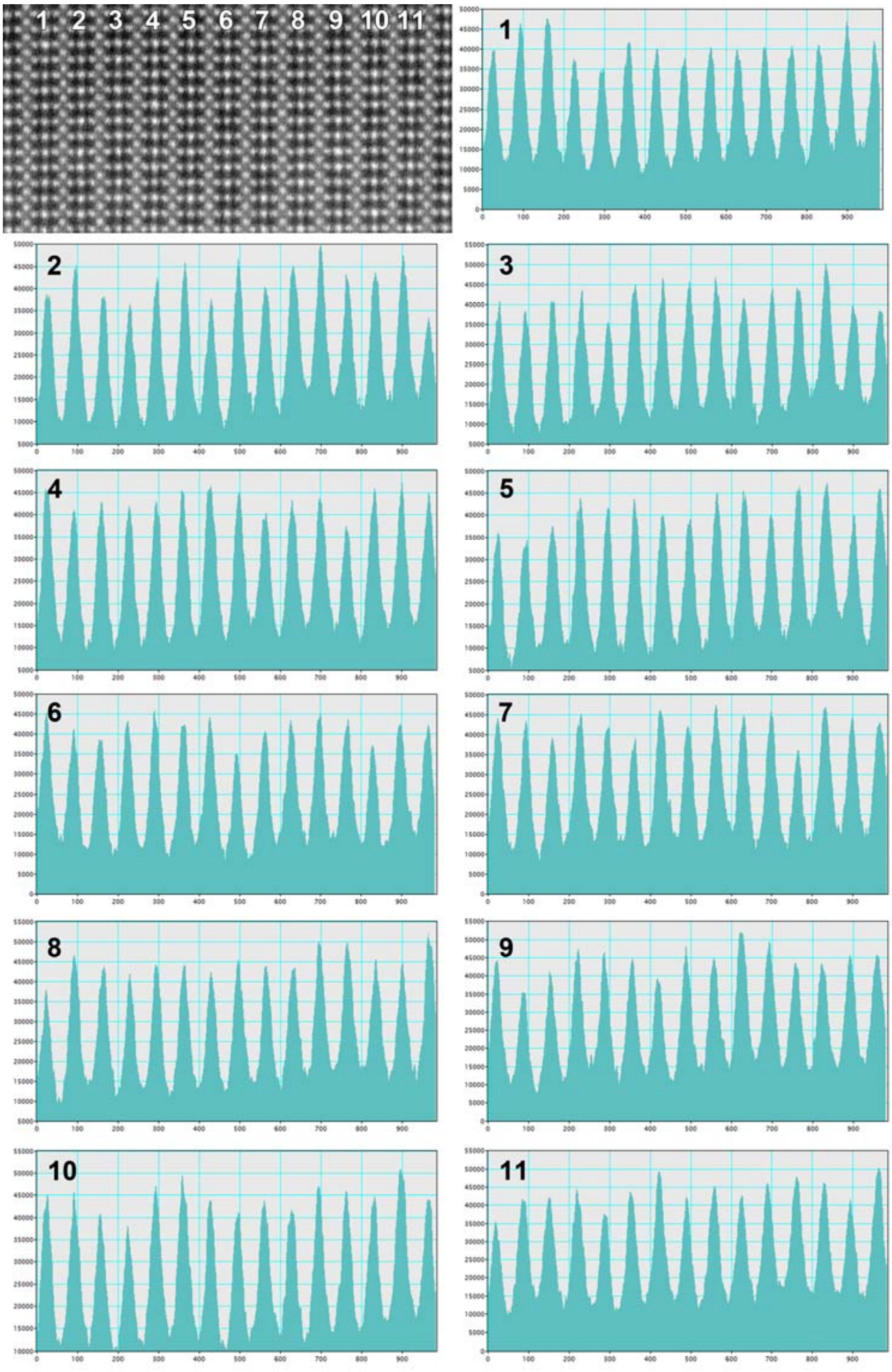

Figure S9. Enlarged [110] HAADF-STEM image for the $Ba_{0.6}K_{0.4}Fe_2As_2$ sample with marked layers 1-11 and the corresponding intensity profiles measured along these layers.